

Conformational Free Energy of Lattice Polyelectrolytes with Fixed End Points. 3. The Elastic Properties of a Permanent Network of Lattice Polyelectrolytes

Th. M. A. O. M. Barenbrug^{*,†} and J. A. M. Smit

Leiden Institute of Chemistry, Gorlaeus Laboratories, Leiden University, P.O. Box 9502, 2300 RA Leiden, The Netherlands

Received March 6, 1998; Revised Manuscript Received September 28, 1998

ABSTRACT: In a previous article (part 1: Barenbrug, Th.M. A. O. M.; Smit, J. A. M.; Bedeaux, D. *Macromolecules* 1997, 30, 605) we used Monte Carlo methods to study the properties of lattice polyelectrolytes with fixed endpoints and proposed expressions for the conformational free energy of a single chain. By connecting these chains by means of tetrafunctional cross-links, a simple model network of lattice polyelectrolytes was conceived. Using the total free energy of the gel and the other constituents, we were able to predict equilibrium swelling (part 2: Barenbrug, Th. M. A. O. M.; Bedeaux, D.; Smit, J. A. M. *Macromolecules*, preceding paper in this issue) under a variety of conditions with respect to the salt content and the linear charge density of the chains. The elastic behavior of the gel is described in this paper (part 3) in terms of the shear modulus as a function of the above conditions. We consider two well-defined swelling circumstances for the gel (cases 1 and 2) and compare our findings with recent experimental results.

1. Introduction

Polyelectrolyte gels are known to show remarkable swelling and elastic properties. Recently their theoretical and practical interest as such has been recognized again.¹ In the past many models have been put forward in order to describe the sometimes unexpected behavior of these systems. After early attempts^{2,3} following the pioneering work of Flory, a sequence of theories was developed,^{4–10} starting with the work of Katchalsky, who derived an expression for the electrostatic contribution to the free energy of a network composed of charged Gaussian chains. The latter free energy models are mainly based on single-chain properties and lose therefore some of their validity when chain–chain interactions become important. Recent scaling theories,^{11–13} employing the “blob” picture, describe probably better the interaction between charged polymer segments. However, such a description is only valid for flexible, weakly charged, long chains and does not seem very suitable for those polyelectrolytes whose persistence length is of the same order of magnitude as their length.

Recently (part 2¹⁵), we proposed a model network in which the chains were connected by tetrafunctional cross-links. The chains were simulated either by charged random walks (RWs) or by charged self-avoiding walks (SAWs), whereas for both types of chains the endpoints were fixed. The electrostatic repulsion in the network was described as a sum of intrachain interactions such as in Katchalsky's theory. However, his original theory was improved to incorporate the effect of charge pair interactions on the conformational statistics of the chains (part 1¹⁴). The resulting expressions were used to describe the swelling behavior of a polyelectrolyte gel as a function of the external salt concentration and the

linear charge density of the chains. As our model thus provides the conformational free energy of the network including the electrostatic term, we shall use it here for the description of the elastic properties of a polyelectrolyte gel.

Usually the elasticity of the polyelectrolyte gel is studied in terms of its response to an externally applied deformation: the gel is brought out of equilibrium, e.g., its free energy is increased, and the force driving the system back to equilibrium is studied. Assuming that the network chains deform affinely with the gel, the precise deformation of a chosen network chain depends on its original orientation in the gel. Therefore, during the deformation some chains will be more extended, others less extended, than before. Due to the changes in the end-to-end distances of the network chains the free energy of the network chains increases. The average magnitude of that increase, denoted $\langle(\partial F/\partial R)_T\rangle$, is proportional to the restoring force exerted by the gel. If one assumes that, during the deformation, the gel volume remains constant, the concentration dependent terms in the total free energy do not change and therefore do not contribute to the elastic response of the gel. Solely the conformation free energy mentioned above yields the restoring force, which is responsible for the elastic response of the polyelectrolyte gel.

In this paper we focus on the response of the gel to a small deformation. Customarily, the elasticity of matter is expressed in terms of elastic moduli: proportionality constants between the applied stress and the resulting relative deformation of the sample. Here we study the behavior of the *shear modulus* of the gel as a function of the salt concentration, under two distinct conditions, numbered 1 and 2.

In case 1 the elasticity modulus is calculated for the gel at a constant polymer volume fraction (i.e., at a *constant volume*), but for different *internal* salt concentrations. In this case the gel is not in contact or in thermodynamic equilibrium with a salt solution, but it

* To whom correspondence should be addressed.

[†]Delft University of Technology, Laboratory for Aero- and Hydrodynamics, Rotterdamseweg 145, 2628 AL Delft, The Netherlands.

is allowed to absorb—starting in the dry state—a salt solution of given ionic strength, until the specified polymer concentration is reached (i.e., until a preset swelling volume is attained). The experimental restraint to this case is that the relative extension of the chains at which the modulus is measured (and by which the volume of the gel is determined) cannot be larger than the equilibrium swelling extension of the chains (volume of the gel) at the same *internal* salt concentration.

In case 2 the gel is in contact with an *external* salt solution, and the shear modulus is determined for different, preset values of the salt concentration. Before each measurement is performed, the gel is allowed to reach its equilibrium swelling volume.

Analogous to the path followed in part 2¹⁵ we first derive, in section 2, expressions that describe the elastic properties of an isotropic polymer network, in terms of its shear modulus. In section 3 we present our results. We compare the shear modulus calculated (a) directly from the Monte Carlo simulation data for a lattice polyelectrolyte of 40 segments and (b) by using our variant of Katchalsky's expression for the electrostatic free energy of a charged chain, to study the applicability of the latter for chains with more segments. We then present and discuss the results for gels of longer chains in good and θ -solvent and compare the outcomes for cases 1 and 2 separately. For both these cases we qualitatively and quantitatively compare the predictions from our isotropic lattice polyelectrolyte gel model and experimental results obtained for poly(acrylic acid) (PAA) gels. As recent work on this topic^{11–13} contains the important simplification that the shear modulus and the network pressure are proportional to each other, we also compare our explicit results for the network pressure and for the shear modulus, to check this assumed property. Section 4 contains a discussion and a summary of our findings.

2. Theory

In general terms the elastic behavior of a swollen polyelectrolyte gel is studied by exerting an external pressure on one of the sides of a conveniently shaped gel sample (during a relatively short period of time) and instantaneously measuring the deformation caused by this pressure. We assume that during this deformation the gel volume remains constant, as are, therefore, the ion concentrations and polymer volume fractions. This assumption has two main implications.

First, that concentration dependent pressure contributions such as the Donnan and mixing contributions do not change *during* the measurement. Therefore, the elastic response of the gel to the compression must be supplied solely by the network forces, so that the measurement of the (macroscopic) elasticity of the gel provides a direct insight in the elastic behavior of the network (and therefore of the (microscopic) chains themselves).

Second, that exerting the external pressure, denoted p_{ext} (see Figure 1), results in a small compression of the gel in the direction of p_{ext} (taken in the vertical z -direction) and an expansion of the gel in both perpendicular horizontal (x - and y -) directions, in such a way that its total volume remains constant. In the figure we show this schematically for a cubic section of the gel and somewhat exaggerated to emphasize the points made here. The variable $l (=H/H_0)$ gives the height of

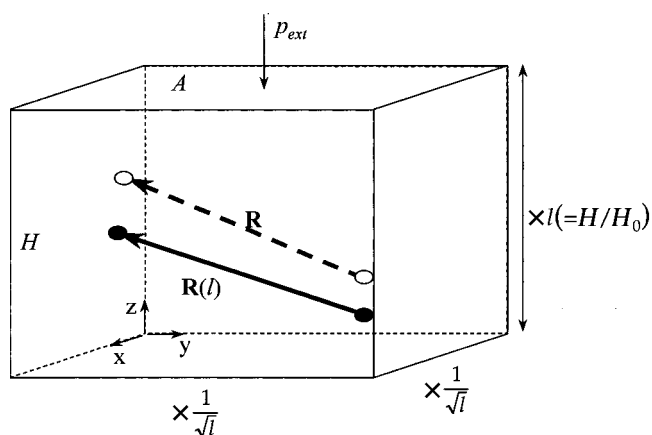


Figure 1. Sketch of the deformation of an arbitrary cubic section of a gel. Shown is the end-to-end vector (arrows) of an arbitrary network chain and the cross-links (circles) it connects, before (dashed \mathbf{R} arrow, open circles) as well as during the deformation (solid $\mathbf{R}(l)$ arrow, filled circles). As indicated, the gel is compressed under an external pressure p_{ext} in the z -direction. $l (=H/H_0)$ is the height of the cube in the z -direction relative to its height before compression. The total volume of the cube is assumed to remain constant ($HA = H_0A_0$); therefore it must expand (we assume symmetrically) in both other directions, by a factor of $1/l^{1/2}$. We assume that the compression induces an affine deformation, with a concomitant affine displacement of the cross-links which connect the end-to-end vectors of the chains. As is indicated, both the directions and the lengths of the end-to-end vectors may change due to this deformation.

the cube, relative to its original height (i.e., its length in the z -direction). Note that, due to the constraint of constant volume and to a basic assumption of symmetry, the horizontal dimensions have become larger (by a factor of $1/l^{1/2}$).

In real gels the orientations of the chains are distributed more or less randomly, instead of forming a certain ideal symmetry. In the following we therefore derive an expression for the shear modulus of an *isotropic* polyelectrolyte gel. Although the assumption of isotropy is more in line with physical reality, at first sight it seems not in agreement with the model of tetrahedrally ordered chains we pictured in part 2.¹⁵ However, we will show that this modification has no implications for the swelling results presented there. Furthermore we use the same notation as in parts 1¹⁴ and 2.¹⁵

Generally, the free energy of the network is the sum of the free energies of the constituent chains (in their respective environments). In the calculation we neglect electrostatic interactions between segments of different polyelectrolyte chains.

For every salt and counterion concentration in the gel, the free energy of a chain, F_{chain} , can be written as a power series in its end-to-end distance R , at least for the relevant range of R values. In this way all deviations from ideal (Gaussian) behavior are also incorporated,

$$\frac{F_{\text{chain}}}{kT} = \sum_{m=0}^{\infty} a_m R^m \quad (2.1)$$

where m is the summation variable and kT has its usual meaning. The values of the a_m are yet to be determined. These depend on the nature of the chain, its length, the segment dimension, the number of charges on the chain's backbone, and the ion concentrations in the gel, while R is determined by the degree of swelling.

We assume, in a first approximation, that the cross-links connect chains of equal length and that they are homogeneously distributed in the gel. Then the end-to-end distances of the N chains incorporated in the network are equal, and, assuming additivity,

$$F_{\text{network}} = NF_{\text{chain}} \quad (2.2)$$

The network pressure, Π_{network} , in swelling equilibrium is given by the negative of the derivative of the free energy with respect to the swelling volume V , the latter being proportional to R^3 ($V = cR^3$, where c is a dimensionless constant). Assuming affine swelling,

$$\begin{aligned} \Pi_{\text{network}} &= -\left(\frac{\partial F_{\text{network}}}{\partial V}\right)_T = -\frac{1}{3cR^2}\left(\frac{\partial F_{\text{network}}}{\partial R}\right)_T \\ &= -\frac{N}{3cR^3}R\left(\frac{\partial F_{\text{chain}}}{\partial R}\right)_T = -\frac{1}{3}\frac{N}{V}kT\sum_{m=0}^{\infty}ma_mR^m \end{aligned} \quad (2.3)$$

With the intermediate results

$$R\left(\frac{\partial F_{\text{chain}}}{\partial R}\right)_T = -Rf \quad (2.4)$$

where f is the tensile force exerted by the chain, we arrive alternatively at the general expression

$$\Pi_{\text{network}} = \frac{1}{3}\frac{N}{V}Rf \quad (2.5)$$

For a network of Gaussian chains, $f/kT = -3R/R_0^2$ (R_0^2 is the mean square end-to-end distance of the Gaussian chain), so that in this case we obtain for the network pressure the well-known result

$$\frac{\Pi_{\text{network}}}{kT} = -\frac{N}{V}\frac{R^2}{R_0^2} \quad (2.6)$$

Equation 2.5 shows that the network pressure is proportional to the chain concentration, the extension of the chains, and the tensile force at this extension. If one calculates N/V , the value of the polymer concentration, using the "unit cube" from Figure 1 of part 2¹⁵ for the calculation and substituting its value in eq 2.5, one obtains eq 2.4.1 of part 2, without explicitly incorporating the orientations of the polyions. The same holds true for the hexafunctional case (see eq 32 of ref 10). For an *isotropic* network containing tetrafunctional cross-links therefore the same swelling behavior is obtained as was found with the explicit descriptions and "ideal" gel structure used in section 2 of part 2. These examples illustrate that knowledge of the functionality of the cross-links in the network, together with the condition of isotropy, is sufficient to determine the values of the concentrations of the different constituents and therefore of the magnitude of the different osmotic pressure contributions, at least in the case of identical network chains.

For the shear modulus G of the isotropic gel of lattice polyelectrolytes we find (see the Appendix for the details of the calculation)

$$\begin{aligned} \frac{G}{kT} &= \frac{1}{3}\frac{N}{V}\sum_{m=0}^{\infty}a_mR^m m\left(\frac{3}{5} + \frac{1}{5}m\right) = -\frac{3}{5}\frac{\Pi_{\text{network}}}{kT} - \\ &\quad \frac{1}{5}\frac{1}{R^2}\frac{\partial}{\partial R}\left(\frac{\Pi_{\text{network}}}{kT}R^3\right) \end{aligned} \quad (2.7)$$

In the last step of the derivation we used that $V \sim R^3$. For Gaussian chains therefore (see eqs 2.3 and 2.6), $G = -\Pi_{\text{network}}$. Generally, if the free energy of the chains can be expressed as a simple scaling law in R , only one of the a_m in the power series is different from zero, and G is still proportional to Π_{network} . However, the proportionality constant is only equal to (minus) one in the case of a pure quadratic relationship (i.e., Gaussian chain behavior). If the dependence of the free energy on R is not a simple scaling law, it can always be described satisfactorily by some polynomial in R (for the relevant range of R values), but in that case G and Π_{network} will generally *not* be proportional.

For an *isotropic* gel of polyelectrolyte chains we can now calculate the shear modulus, for both experimental cases, as described above. For case 1 as well as for case 2 we proceed in the same manner, by first determining the concentrations of the different mobile, charged particles in the gel and from these the inverse Debye screening length, κ , using the expressions for the different contributions to the osmotic pressure in the gel (see section 2 of part 2¹⁵). Then we determine the tensile force exerted by the chains in this medium, as a function of R (see sections 2.2–4 of part 2), without changing the properties of the medium during the latter process, as we assume that neither the degree of swelling nor the composition of the internal medium changes as a result of the brief and small compression that is applied to measure the network's elastic response. The R dependence of the tensile force obtained is then used to calculate the fit parameters a_m . By substituting these values and the correct value of R into (2.7) the value of the shear modulus is found.

Following this approach, the difference between cases 1 and 2 lies solely in the difference in the determination of κ and of the value of R used for the calculation of G . In case 1 the concentrations of the small ions in the gel are imposed and determine the value of κ . The shear modulus is then calculated for different salt concentrations *in* the gel, at constant volume, i.e., at one fixed value of R . In case 2 the salt concentration in the external solution determines the equilibrium degree of swelling (and therefore the value of R) and, via the Donnan osmotic pressure term, the internal salt concentration, C_s , and therefore the value of the Debye screening length in the gel. The shear modulus is then calculated for different *external* salt concentrations, with the corresponding equilibrium values of R and C_s .

As mentioned, the degrees of swelling to be used for the calculations to describe case 1 must be lower than all equilibrium degrees of swelling attained in case 2, for the range of salt concentrations considered. In the case of a real gel, the intrinsic stiffness of the chains is higher than in our model (and therefore the equilibrium extension of the chains is higher). We therefore have used somewhat higher values for the (fixed) parameter x in the figures illustrating case 1. We will return to this point later.

3. Results

3.1. General. In this section we present the results found for the shear modulus of a model polyelectrolyte gel, consisting of tetrahedrally ordered, cross-linked lattice polyelectrolyte chains. The moduli are calculated by first determining the relative extension $x (=R/L)$ of the chains, where their contour length L is equal to na ; the number of links, n , between the $n + 1$ segments, times the bond length a . For case 1 this value is preset; for case 2 that x value is determined, for which the total (osmotic) pressure of the gel equals zero ($\Pi = 0$; see section 2 of part 2,¹⁵ also for what follows) for the given external salt concentration. With the obtained value of x the concentrations of the different constituents of the gel can be calculated and consequently the magnitude of the tensile force exerted by the network chains. As during the elasticity measurement these concentrations do not change, the R dependence of the tensile force of a single chain can easily be determined. Finally, the use of eqs 2.5 and 2.7 gives the shear modulus of the gel.

In section 3.2 we compare the shear modulus calculated (a) directly from the Monte Carlo simulation data for a lattice polyelectrolyte of 40 segments and (b) using our variant of Katchalsky's expression for the electrostatic free energy of a charged chain (eqs 2.3.2a,b in part 2¹⁵), to obtain an indication of the accuracy of the latter approach. In sections 3.3–3.6 case 1 is studied. In section 3.3 we present and discuss the results for gels of longer chains in good (athermal) solvent and θ -solvent, modeled by networks of charged SAW and RW chains, respectively, where we use our Katchalsky variant for the pairwise electrostatic interactions between the charged segments within a single network chain. Some characteristic differences in the behavior of the model gel, for both (limiting) solvent conditions, are discussed. In section 3.4, the results are quantitatively compared to experimental results for PAA gels. In section 3.5 we compare our results for the network pressure and for the shear modulus. In the same way, sections 3.6–3.8 contain a treatment of case 2.

In experimental situations the solvent quality usually depends on the ionic strength. At very high salt concentrations, the solvent might even become so strongly polar that the polyelectrolyte precipitates ("salts out"). In this paper only both limiting cases, good solvent and θ -solvent, are studied, and the above salt effect is not taken into account. Results are presented for linear charge densities up to the counterion condensation threshold according to Manning, i.e., at a linear charge density of 35% in our model.

For consistency, in all figures and calculations presented for either SAW chains (good solvent) or RW chains (θ -solvent), the values of the relevant parameters were adapted to either case (see part 2¹⁵): the Flory–Huggins interaction parameter χ was set to 0 and 0.5, respectively,¹⁶ and h_0^2 , the most probable value of the squared end-to-end distance of the chain, was given a value of $(2/3)\langle R_0^2 \rangle$ for respectively the SAW or the RW chain under consideration (see Table 3 in part 1¹⁴).

3.2. Modulus of a Gel of Short Chains. Direct Calculation with MC Data. In Figure 2 we plotted for comparison both the shear modulus of a lattice polyelectrolyte gel of chains of 40 segments, calculated directly from the Monte Carlo data for the free energy of a lattice polyelectrolyte with fixed endpoints, and the values for the shear modulus of the same system,

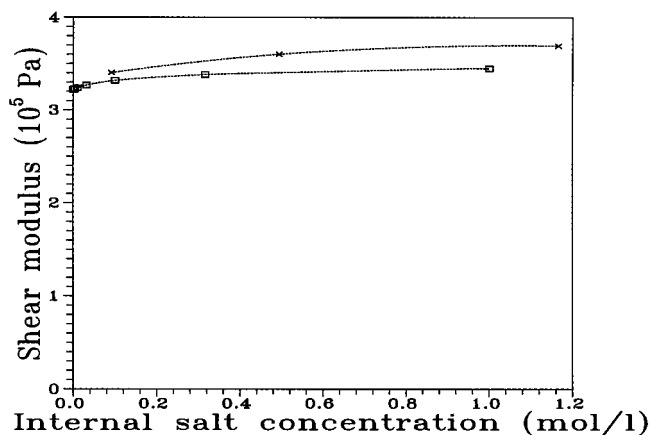


Figure 2. Plot of the shear modulus of a lattice polyelectrolyte gel versus the internal salt concentration, at a constant gel volume (case 1; $x = 0.5$; the monomer concentration is 0.7 mol/L), for chains of 40 segments. The linear charge density is 30%. Results calculated directly from the Monte Carlo data (x) for $\kappa a = 0, 0.3, 0.6$, and 0.9 and results from the modified expression of Katchalsky (\square) are shown. The dotted curves are added as a guide to the eye.

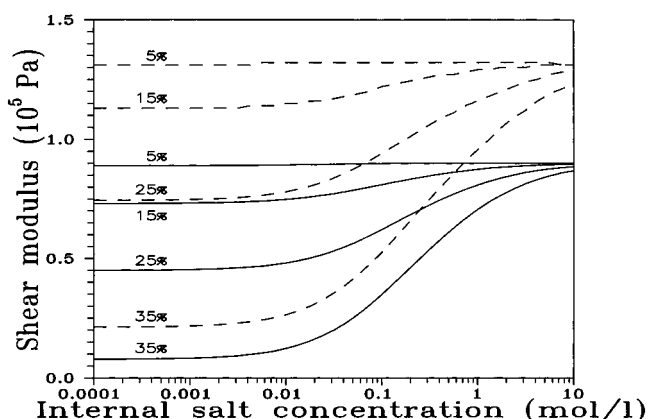


Figure 3. Plot of the shear modulus of a gel of charged SAWs (solid curves) and RWs (dashed curves) of 80 segments, versus the salt concentration in the gel, for different linear charge densities, as indicated in the figure. The swelling volume of the gel is constant (case 1). For the fixed relative extension of the chains we have chosen $x = 0.4$ (the monomer concentration is 0.34 mol/L).

calculated by using the modified expression of Katchalsky for the free energy of the charge interactions (see eqs 5.4a–c of part 1¹⁴ and eqs 2.3.2 of part 2¹⁵). As, for every chain length, we performed simulations for three different values of the inverse Debye screening length, κ , the Monte Carlo results cover only three separate points in the figure. Besides, as we only have simulation results for relatively high values of κ , there is not much salt dependence to be observed. Nevertheless the agreement between the results of both methods is satisfactory: relative errors, also for the other attainable values of x and q , the number of charges on the chain, are smaller than 10% (results are not shown).

3.3. Shear Modulus of Gels of Longer Chains

Case 1. In Figure 3 we plotted the results found for the shear modulus of an isotropic model gel of lattice polyelectrolyte chains of 80 segments at constant gel volume (case 1), as a function of the internal salt concentration, both for a gel of SAW chains and a gel of RW chains. The different curves represent the results for different linear charge densities, $q/(n + 1) \times 100\%$, as indicated in the figure. From here on we take for the

electrostatic contribution the modified expression of Katchalsky, assuming that the relative error in the results will be of the same order of magnitude (around 10%) as found in the previous subsection.

We observe that in general the shear modulus of SAWs is, for the same relative extension, (much) smaller than for RWs. This is due to the fact that the tensile force exerted by the RWs is, at the same relative extension, much higher than in the SAW case, as we also observed in sections 2.2 and 3 of part 2.¹⁵ Generally this leads to higher network pressures in the case of RWs (see eq 2.5). As globally the shear modulus follows more or less the network pressure (cf. eq 2.7) this also leads to higher values for G .

For increasing linear charge density, the shear modulus decreases; the relative effect of charging is more or less the same for RW and SAW chains. For a clear understanding of the influence of the charge interactions on the elastic modulus of the gel, it is helpful to describe the network chains in terms of equivalent Kuhn chains, which consist of cylindrical segments that exhibit only hard-core interactions. The length and the diameter of these Kuhn segments follow directly from the stiffness and the segmental excluded volume, caused by the magnitude and the nature of the segment-segment interactions in the original chain. If the charge density on the network chains is increased, the repulsive interactions between the segments are enhanced, so that the chain becomes stiffer and its electrostatic excluded volume becomes larger. Therefore, the segments of the equivalent Kuhn chain become longer and thicker. However, their number must decrease, as the chain length itself remains the same. Having less Kuhn segments and therefore less conformational freedom, the network chains have a lower entropy and thus exert smaller tensile forces on the network. As the tensile forces are reduced, the network pressure (see eq 2.5) and thus the shear modulus (cf. eq 2.7) must decrease. Consequently, the modulus of the gel decreases as a function of the linear charge density.

Near 35% linear charge density and for low salt concentration, the electrostatic excluded volume clearly dominates the bare excluded volume contribution of the SAWs, so that the elastic behavior of RW and SAW chains converges. If the salt concentration increases, the electrostatic interactions are screened more effectively, and the curves for different charge densities converge to what can be understood as the shear modulus of the corresponding uncharged network. The scaling theories^{11,12} mentioned do not explicitly contain this screening effect, as they lack the explicit effect of the charge interactions on the chain statistics (see ref 12, Figure 7).

3.4. Quantitative Comparison with Experimental Results. Case 1. Comparison of our results for G at constant swelling volume (Figure 3) with the experimental outcomes (Figure 4) shows a clear qualitative agreement, including the effect of charging and the convergence of the curves for higher salt concentrations. Note that much higher internal salt concentrations are not experimentally accessible: the gel will not absorb large enough quantities to attain the preset swelling volume. For the quantitative discrepancies between Figures 3 and 4 there are two reasons.

First, we must take the effect of a higher intrinsic chain stiffness into account, as compared to the value used in the Monte Carlo simulations (see also part 2,¹⁵

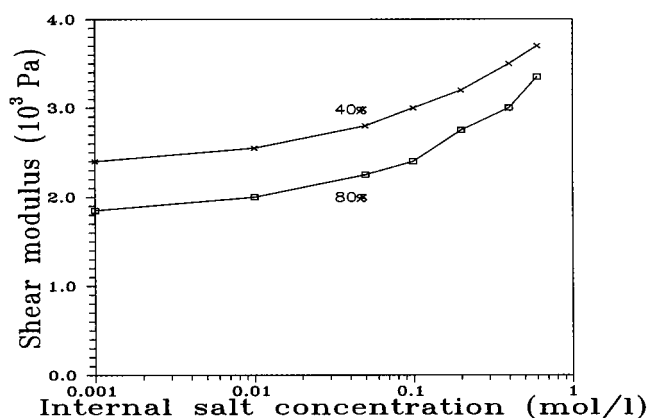


Figure 4. Experimental results¹⁷ for the shear modulus of a PAA gel at constant swelling volume (case 1) versus the internal salt concentration. Shown are the results for two different values of the linear charge density (indicated in the figure). The cross-link density is 2%. The monomer concentration is 0.916 mol/L. The straight lines are added as a guide to the eye.

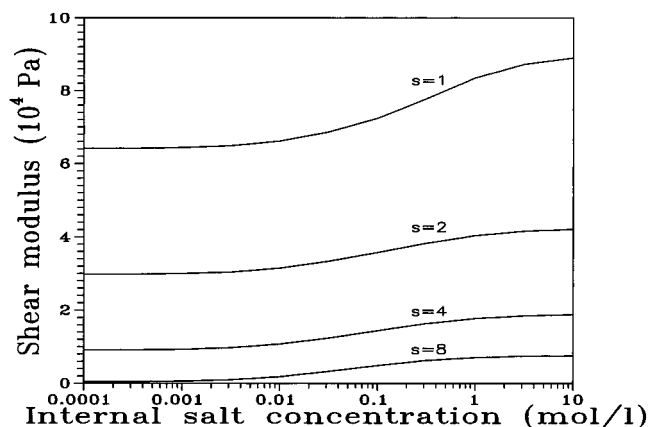


Figure 5. Shear modulus of a lattice polyelectrolyte gel of RW chains of 80 segments, with different values of the Kuhn segment length (indicated in the figure; s is the number of chain segments per Kuhn segment), calculated at constant gel volume (case 1; $\chi = 0.7$). The linear charge density is 35%.

section 3.4). To show the effect of larger intrinsic persistence lengths on the shear modulus of the gel, we calculated this quantity for a gel of RW chains of 80 segments at constant gel volume and for different values of the parameter s , the number of chain segments per Kuhn segment, following the same procedure as in part 2. The results are shown in Figure 5. Note that, to obtain physically meaningful values for G , we took a higher value ($\chi = 0.7$) for the relative extension of the chains than was taken in Figure 3, which corresponds to their stiffer behavior. One sees that for s values of about 8 the values calculated for G fall within the experimentally observed range. This s value agrees with the experimental result for the intrinsic stiffness of PAA chains. Also the salt concentration dependence agrees well with experiment (see Figure 4).

A second source for the discrepancy between theory and experiment is the restriction in our model to linear charge densities not higher than 35%. Strictly this percentage is found by using Manning's condensation concept in which the PAA chain is simplified to a line charge. It may be argued that for real chains condensation might take place at higher linear charge densities.

Clearly, establishing a more rigorous quantitative agreement without using adaptable parameters is not

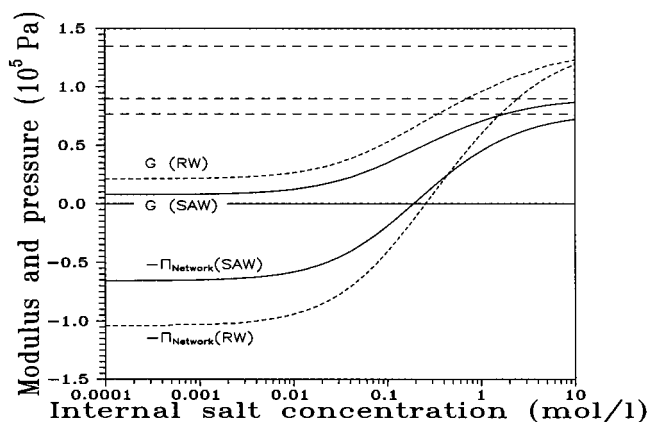


Figure 6. Comparison of shear modulus (G) and network pressure (Π_{network}) both for a gel of SAW chains (solid) and for a gel of RW chains (short dashes) of 80 segments, as a function of the internal salt concentration, at constant gel volume (case 1). The linear charge density is 35% and the relative extension of the chains, $\alpha = 0.4$. For a comparison the limiting values of the shear modulus and the network pressure of the uncharged chains are added (longer dashes). RW results: upper horizontal dashed line ($-\Pi_{\text{network}, q=0, \text{RW}} = G_{q=0, \text{RW}}$). For SAWs these limiting values do not converge: middle dashed line, $G_{q=0, \text{SAW}}$, and lowest dashed line, $-\Pi_{\text{network}, q=0, \text{SAW}}$.

possible, as there exist many uncertainties regarding different descriptive parameters of the real gel (e.g., the effective cross-link density and thus the average chain length between cross-links, the chain length distribution, the precise Manning condensation threshold and thus the effective linear charge density, etc.).

3.5. Comparison of Network Pressure and Shear Modulus. Case 1. In Figure 6 we plotted, for a comparison, the value of the shear modulus and of the network pressure versus the internal salt concentration, at constant gel volume (case 1), for both types of chains. The figure shows clearly that for the chosen example G and $-\Pi_{\text{network}}$ are neither equal nor proportional to each other. In particular for low salt concentrations (i.e., high charge interactions) we see that G and Π_{network} even have the same sign. For these small values of the internal salt concentration the network pressure is positive: the network prefers to swell. For high salt concentrations the charge effects are screened, and the network pressure becomes negative.

In case 1 the network pressure is only compensated by the mixing term (there is no external salt solution and therefore no Donnan osmotic pressure contribution), so that at very high internal salt concentrations the network pressure would be so strongly negative, that the mixing term could not compensate for its influence: the gel would spontaneously release some of its internal fluid and could not be kept at the preset fixed volume. This is why the experimental curves in Figure 4 stop in the range of salt concentrations of around 1 mol/L.

Nevertheless, the theoretical curves in Figure 6 are also plotted for higher internal salt concentrations. One sees that for these high salt concentrations the curves for the shear modulus and the (negative) network pressure of the relatively long RW chains asymptotically approach the same limiting curve for the Gaussian chain; for the gel of SAW chains these curves do not converge, as we expect (eq 2.7). Both limiting curves for the bare network pressure and for the shear modulus of an uncharged network of SAW chains are plotted in the graph (long dashes). As the gel volume is kept constant (case 1) these curves are horizontal lines.

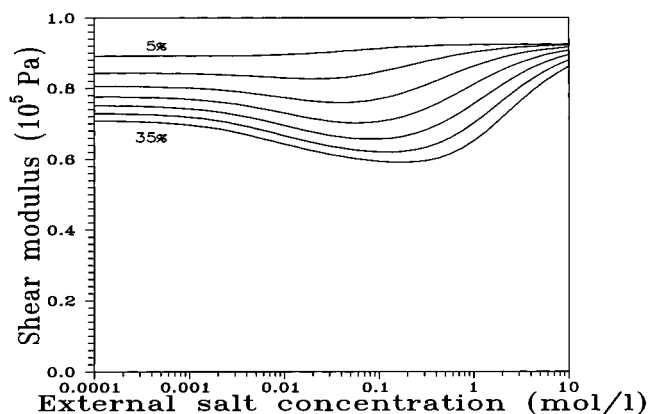


Figure 7. Plot of the shear modulus of a lattice polyelectrolyte gel of charged SAWs of 80 segments, versus the external salt concentration, for different linear charge densities, as indicated in the figure. The gel is in equilibrium with the surrounding salt solution (case 2).

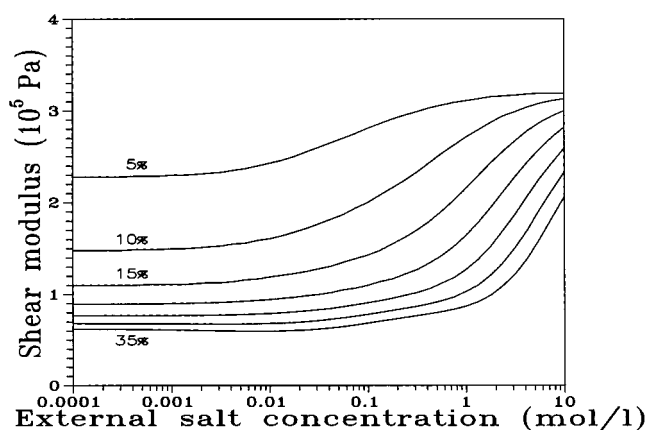


Figure 8. As Figure 7, but now for a gel of RW chains.

3.6. Shear Modulus of Gels of Longer Chains. Case 2. In Figures 7 and 8 we plotted the results found for the shear modulus of a polyelectrolyte gel in thermodynamic (Donnan) equilibrium with a surrounding salt solution (case 2), both for SAWs and RWs, versus the external salt concentration. As in case 1 we observe that the shear modulus approaches a certain limiting, maximum value for high external salt concentrations, which can be understood as the shear modulus of the uncharged, swollen gel. We also observe a large difference in magnitude between the moduli of the gel in good solvent and in θ -solvent. Furthermore, the shear moduli also decrease with increasing linear charge density.

However, comparing case 1 and case 2 we observe two large differences. In case 2, the effect of increasing the linear charge density on the value of G is much larger for RWs than for SAWs, whereas in case 1 the relative effect was seen to be more or less the same for both chain types. This can be understood by a comparison of the swelling results in Figures 6 and 7 of part 2,¹⁵ for the case of equilibrium swelling: in the case of θ -solvent the gel shows a much stronger swelling upon charging than in the good solvent case. Therefore, the introduction of (a few) charges leads to a much stronger effect on the excluded volume of the RW chain than in the corresponding SAW case and thus on its degrees of freedom. Further, in the case of θ -solvent the chain concentration shows much larger changes upon charging, which directly affects the shear modulus (see eq 2.7). The other clear difference between the results for

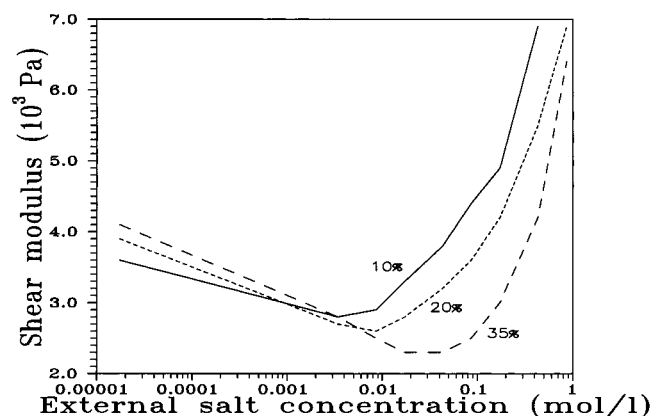


Figure 9. Experimental results¹⁷ for the shear modulus of PAA gels in equilibrium with a surrounding salt solution, versus the external salt concentration, for different values of the linear charge density (indicated in the figure). The cross-link density is 2%. For clarity the data points are connected by straight lines as a guide to the eye.

case 1 and case 2 is the effect on G of adding more charge to the chains. In case 2 the incremental effect of adding extra charge to the chains becomes smaller at higher linear charge densities, while in case 1 the effect of adding extra charge is more important for high values of the linear charge density. This is caused by the reciprocal relationship between the chain concentration and the degree of swelling (see Figures 6 and 7 of part 2¹⁵).

The influence of the linear charge density on the value of G is a bit blurred by the nonmonotonic salt concentration dependence, as for intermediate salt concentrations, and particularly for the good solvent case, the shear modulus of the polyelectrolyte gel shows a minimum value which becomes more pronounced and shifts toward higher salt concentrations for increasing linear charge densities. In θ -solvent these minima are much less significant; they occur at lower salt concentrations and appear only for high values of the charge density.

3.7. Brief Comparison with Experiment. Case 2. In Figure 9 we plotted, for a comparison, experimental results¹⁷ for the shear modulus of a PAA gel in swelling equilibrium (case 2), as a function of the external salt concentration for different values of the linear charge density. The results agree qualitatively with Figure 7, including the predicted minima in G that, for increasing charge density become more pronounced and shift toward higher salt concentrations. For external salt concentrations around 10^{-3} mol/L, we observe a crossover in the experimental values that does not appear in the calculations. However, at these low salt concentrations and in particular for high charge densities, the charge interactions become very strong and our modified Katchalsky description in which higher order charge interactions are neglected loses its validity.

One also observes, that the theoretical predictions are much too high. Thus, like before, a stiffness correction is necessary to get better quantitative agreement between theory and experiment.

The experimental results indicate that at low salt concentration the real PAA chains behave more like SAWs, as these show distinct minima in the value of G versus the salt concentration. At high salt concentrations G increases strongly with the salt concentration, which is just observed for RWs. This might be due to a decrease of the solvent quality with increasing salt concentration ("salting-out" of PAA).

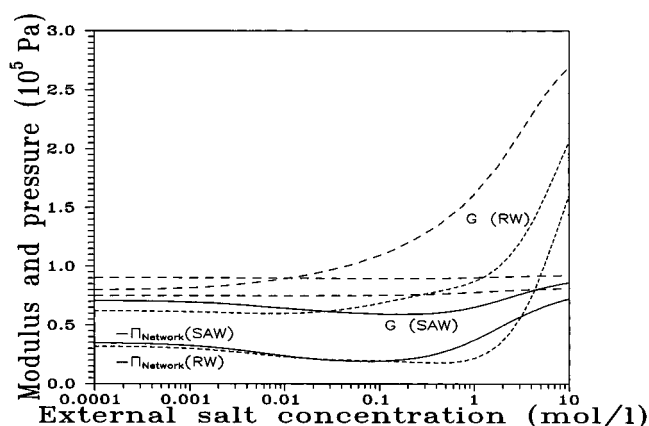


Figure 10. As Figure 6, but now for a lattice polyelectrolyte gel in equilibrium with an external salt solution (case 2). Note that in this case the limiting values for G and $-\Pi_{\text{network}}$ (for $q = 0$) depend on the relative extension x via the swelling volume and thus via the external salt concentration. The steep limiting curve ($G_{q=0,\text{RW}} = -\Pi_{\text{network},q=0,\text{RW}}$) is for a gel of uncharged RW chains. The other, more or less horizontal curves are for the gel of uncharged SAW chains ($G_{q=0,\text{SAW}}$ and $-\Pi_{\text{network},q=0,\text{SAW}}$).

3.8. Comparison of Network Pressure and Shear Modulus. Case 2. In Figure 10 we plotted the calculated shear moduli and the negative of the network pressures, for both types of fully charged gels, in equilibrium with an external salt solution. As we have also seen for case 1 (cf. Figure 6), neither for the good solvent case nor for the θ -solvent case, the $-\Pi_{\text{network}}$ of the lattice polyelectrolyte gel is really proportional to the shear modulus G , although for higher external salt concentrations both quantities show roughly the same behavior as a function of the salt concentration. Further we observe that the behavior of the gel of charged RW chains follows roughly the trends seen for the limiting Gaussian chain (upper dashed curve). However, the behavior is definitely not completely the same, for the range of salt concentrations covered. Due to the collapse of the chains in this case and the concomitant higher values of the segment and counterion concentration, differences with the Gaussian behavior are much larger than in case 1, and for the case of RW chains we do not see a clear convergence to the Gaussian limiting curve. As in case 1, the curves of $-\Pi_{\text{network}}$ and of G of the gel of SAW chains do not converge for high salt concentrations. The limiting curves (for $q = 0$) for these quantities are both plotted (longer dashes).

4. Conclusions

The shear modulus G of the lattice polyelectrolyte gel has been studied for two cases: 1 at constant swelling volume and at given *internal* salt concentration and 2 in swelling equilibrium with an *external* salt solution of given concentration. Within the framework of our approach we did not revert to the simple relationship $G = -\Pi_{\text{network}}$, which is supposed in many theories,^{11–13,18} but which is only true for uncharged Gaussian chains. We derived a general analytical expression (eq 2.7) which establishes the relationship between the shear modulus and the network pressure in an isotropic gel composed of equal chains. This expression shows, that only if the network pressure depends as a simple scaling law on the end-to-end distance, the shear modulus is proportional to the network pressure. Consequently we found (Figures 6 and 10) that the shear modulus and

the network pressure of our model gel globally follow the same trend but are not proportional to each other.

The shear modulus is a measure for the change in the average tensile pressure exerted by the network chains, as a function of the relative deformation of the gel. G is therefore directly related to the change in the conformational degrees of freedom of the network chains caused by the deformation. If the charge interactions between the network chain segments are increased, the Kuhn segment length of these chains and the effective excluded volume of the Kuhn segments is enhanced. As a result the equivalent Kuhn chains have fewer, longer, thicker segments. If the network of these charged chains is then deformed, less degrees of freedom are lost than in the corresponding uncharged case. Therefore the modulus of the gel *decreases* as a function of the linear charge density: the stronger the charge interactions, the softer the gel (see Figures 3, 7, and 8). This is in agreement with experimental results (Figures 4 and 9).

If the salt concentration is increased, case 1 and case 2 give different results. In case 1 the modulus of the gel decreases with increasing salt concentration, because charge interactions are screened, whereas in case 2 the latter effect is masked by the collapse of the gel, during which electrostatic effects become stronger, leading to a minimum value in G , particularly in good solvent. For increasing linear charge density this minimum becomes more manifest, and its position shifts to higher salt concentrations (Figure 7). Qualitatively, this result agrees with experimental findings (Figure 9). For the θ -solvent case only flat minima are predicted for high charge densities, which vanish at higher salt concentrations (Figure 8). For very high salt concentrations the modulus attains a limiting value, irrespective of the linear charge density, which corresponds to the modulus of the uncharged network. Therefore, study of elastic behavior in swelling equilibrium (case 2) at low salt concentration reveals differences between RWs and SAWs in the network, which have not been observed in the swelling equilibrium itself. In swelling equilibrium one observes only Π_{network} , whereas in the shear modulus the combination of this quantity and its derivative with respect to R is seen. At high extensions SAWs and RWs differ not from each other through Π_{network} but they do through $\partial\Pi_{\text{network}}/\partial R$. In this sense elastic behavior just provides additional insight in the influence of the solvent quality on gel properties.

The values for G that are obtained for the model gels are 1–2 orders of magnitude higher than the values measured for PAA gels. This difference stems from the high flexibility of the lattice chains. By increasing the Kuhn length of the bare lattice chains and adapting the intrinsic stiffness in the modified expression of Katchalsky to the values found for PAA, we showed for the case of RW chains that the calculated values of G decrease to realistic values (Figures 4 and 5). This correction is the same as has been used in the description of swelling (part 2¹⁵).

In conclusion, the theory described here consistently and explicitly accounts for the interactions between the charges on the chain, their influence on its behavior, and the salt dependence of these interactions. Most of the gel models used currently lack this important correction, as they are either based on Katchalsky's description of the electrostatic contribution to the free energy or based on scaling relations which contain only implicit fit parameters to account for this charge effect

in an averaged way. As a result our model describes the experimental data in a semiquantitative way.

Acknowledgment. Th.M.A.O.M.B. acknowledges support by the Koninklijke/Shell Laboratories, Amsterdam.

Appendix

In this Appendix we calculate the shear modulus of a swollen, isotropic gel of lattice polyelectrolytes, connected by tetrafunctional cross-links.

In the swollen, undeformed, and isotropic gel we assume the end-to-end vectors of the chains to have all possible orientations but their lengths to be equal. Therefore we can write for the end-to-end vector of chain i before the deformation

$$\mathbf{R}_i = (R_{i,x}, R_{i,y}, R_{i,z}) = R(\sin \vartheta_i \cos \varphi_i, \sin \vartheta_i \sin \varphi_i, \cos \vartheta_i) \quad (\text{A.1})$$

as the value of R is the same for all chains, but the ϑ_i and φ_i of the different chains have such values that the \mathbf{R}_i are distributed randomly in the isotropic gel.

When the gel is deformed by a factor of l in one direction (for convenience we use a compression in the z -direction), the change of the end-to-end distances of the constituent chains and of their orientations will depend on their original orientation. Assuming that the whole of the gel deforms affinely and that its volume remains constant, we can write for the end-to-end vector $\mathbf{R}(l)_i$ during the deformation

$$\mathbf{R}(l)_i = (R(l)_{i,x}, R(l)_{i,y}, R(l)_{i,z}) = R \left(\frac{1}{l^{1/2}} \sin \vartheta_i \cos \varphi_i, \frac{1}{l^{1/2}} \sin \vartheta_i \sin \varphi_i, l \cos \vartheta_i \right) \quad (\text{A.2})$$

As, generally, during the deformation the free energy of different chains will not be equal anymore but will depend on their original orientations, we must average the expression for the free energy over all possible *original* orientations of the chains. Here we need the assumption that the gel is isotropic, so that all original orientations of the \mathbf{R}_i have the same probability. For the free energy of the gel during the deformation we obtain (see eqs 2.1–2; in the averaging process we drop the subscript i),

$$\frac{F_{\text{network}}}{kT} = N \sum_{m=0}^{\infty} a_m \langle |\mathbf{R}(l)|^m \rangle \quad (\text{A.3})$$

where $||$ and $\langle \rangle$ denote respectively the length of a vector and the average over all possible values of ϑ and φ . Using that

$$\begin{aligned} |\mathbf{R}(l)_i|^2 &= R^2 \left(\frac{1}{l} \sin^2 \vartheta_i \cos^2 \varphi_i + \frac{1}{l} \sin^2 \vartheta_i \sin^2 \varphi_i + l^2 \cos^2 \vartheta_i \right) \\ &= R^2 \left(\frac{1}{l} \sin^2 \vartheta_i + l^2 \cos^2 \vartheta_i \right) \end{aligned} \quad (\text{A.4})$$

we find for the free energy during deformation,

$$\begin{aligned}
 \frac{F_{\text{network}}}{kT} &= N \sum_{m=0}^{\infty} a_m \langle [|\mathbf{R}(l)|^2]^{m/2} \rangle \\
 &= N \sum_{m=0}^{\infty} a_m R^m \left\langle \left(\frac{1}{l} \sin^2 \vartheta + l^2 \cos^2 \vartheta \right)^{m/2} \right\rangle \\
 &= N \sum_{m=0}^{\infty} a_m R^m \left\{ \frac{1}{2} \int_0^\pi \left(\frac{1}{l} \sin^2 \vartheta + l^2 \cos^2 \vartheta \right)^{m/2} \sin \vartheta d\vartheta \right\} \\
 &= N \sum_{m=0}^{\infty} a_m R^m \left\{ \frac{1}{2} \int_{-1}^1 \left(\frac{1}{l} (1-t^2) + l^2 t^2 \right)^{m/2} dt \right\} \\
 &\equiv N \sum_{m=0}^{\infty} a_m R^m \gamma(l, m) \quad (\text{A.5})
 \end{aligned}$$

where we substituted $t \equiv \cos \vartheta$. The expression between braces, in the following denoted $\gamma(l, m)$, can be calculated explicitly,¹⁹

$$\gamma(l, m) = \frac{1}{l^{m/2}} \sum_{r=0}^{m/2} \frac{1}{2r+1} \frac{\left(\frac{m}{2}\right)!}{r! \left(\frac{m}{2} - r\right)!} (l^3 - 1)^r \quad \text{for } m \text{ even}$$

and

$$\begin{aligned}
 \gamma(l, m) &= \frac{1}{l^{(m-3)/2}} \sum_{r=0}^{(m-1)/2} \frac{m! (r!)^2}{2^{m-2r} \left(\frac{m+1}{2}\right)! \left(\frac{m-1}{2}\right)! (2r+1)!} l^{\beta r} + \\
 &\dots + \frac{m!}{l^{m/2} (l^3 - 1)^{1/2} 2^{m+1} \left(\frac{m-1}{2}\right)! \left(\frac{m+1}{2}\right)!} \times \\
 &\quad \ln \left[\frac{l^{\beta/2} + (l^3 - 1)^{1/2}}{l^{\beta/2} - (l^3 - 1)^{1/2}} \right] \quad \text{for } m \text{ odd} \quad (\text{A.6})
 \end{aligned}$$

where the analytical functions may take complex values (for $l < 1$), but the final outcomes are always real. In this treatment the degree of swelling and the deformation of the gel have been separated; the end-to-end distance R takes the equilibrium degree of swelling of the gel into account, while the deformation of the gel is contained in the relative extension parameter, l .

The gel is deformed due to the influence of the external force f_{ext} on the gel, which can be calculated by taking the spatial derivative of the free energy with respect to the deformation itself,

$$f_{\text{ext}} = - \frac{\partial F_{\text{network}}}{\partial H} = - \frac{1}{H_0} \frac{\partial F_{\text{network}}}{\partial l} \quad (\text{A.7})$$

where H_0 is the linear dimension of the gel sample before deformation, measured along the direction of the external force (see Figure 1). We find, using (A.5),

$$\frac{f_{\text{ext}}}{kT} = - \frac{N}{H_0} \sum_{m=0}^{\infty} a_m R^m \frac{\partial \gamma(l, m)}{\partial l} \quad (\text{A.8})$$

The pressure exerted by f_{ext} acts on the top area, A , of the gel sample (see Figure 1), so that we find for the pressure

$$p_{\text{ext}} = \frac{f_{\text{ext}}}{A} = \frac{l f_{\text{ext}}}{A_0} = - kT \frac{N}{V} \sum_{m=0}^{\infty} a_m R^m l \frac{\partial \gamma(l, m)}{\partial l} \quad (\text{A.9})$$

Note that we used here that $H = lH_0$ and $A = A_0/l$, as the volume of the sample remains constant: $HA = H_0A_0$.

Young's modulus of elasticity is defined as $E = -[\partial p_{\text{ext}}/\partial l]_{l=1}$, i.e., the proportionality constant for the increase of the pressure with the relative compression, in the limit of very small deformations. The shear modulus, G , of the gel is proportional (with a factor of 1/3 for this incompressible system²⁰) to its Young's modulus E , so that

$$\frac{G}{kT} = \frac{1}{3} \frac{N}{V} \sum_{m=0}^{\infty} a_m R^m \left[\frac{\partial \gamma(l, m)}{\partial l} + l \frac{\partial^2 \gamma(l, m)}{\partial l^2} \right]_{l=1} \quad (\text{A.10})$$

Using the integral expression between braces in eq A.5 for $\gamma(l, m)$, we can differentiate under the integral sign with respect to l and substitute $l = 1$. Then performing the remaining integral we obtain eq 2.7.

References and Notes

- (1) De Rossi, D.; Kajiwar, K.; Osada, Y.; Yamauchi, A. *Polymer Gels*; Plenum: New York, 1991. Many other examples are given in: *Adv. Polym. Sci.* **1993**, *110*.
- (2) Katchalsky, A. *J. Polym. Sci.* **1951**, *7*, 393.
- (3) Hill, T. L. *J. Chem. Phys.* **1952**, *20*, 1259.
- (4) Katchalsky, A.; Lifson, S. *J. Polym. Sci.* **1953**, *11*, 409.
- (5) Katchalsky, A.; Michaeli, I. *J. Polym. Sci.* **1955**, *15*, 69.
- (6) Hasa, J.; Ilavsky, M.; Dusek, K. *J. Polym. Sci., Polym. Phys. Ed.* **1975**, *13*, 253.
- (7) Ilavsky, M. *Polymer* **1981**, *22*, 1687.
- (8) Ohmine, I.; Tanaka, T. *J. Chem. Phys.* **1982**, *77*, 5725.
- (9) Ilavsky, M. *Adv. Pol. Sci.* **1993**, *109*, 173.
- (10) Barenbrug, Th. M. A. O. M.; Smit, J. A. M.; Bedeaux, D. *Polym. Gels Networks* **1995**, *3*, 331.
- (11) Dobrynin, A. V.; Colby, R. H.; Rubinstein, M. *Macromolecules* **1995**, *28*, 1859.
- (12) Rubinstein, M.; Colby, R. H.; Dobrynin, A. V.; Joanny, J.-F. *Macromolecules* **1996**, *29*, 398.
- (13) Barrat, J.-L.; Joanny, J.-F. *Adv. Chem. Phys.* **1996**, *94*, 1.
- (14) Barenbrug, Th. M. A. O. M.; Smit, J. A. M.; Bedeaux, D. *Macromolecules* **1997**, *30*, 605 (part 1).
- (15) Barenbrug, Th. M. A. O. M.; Bedeaux, D.; Smit, J. A. M. *Macromolecules*, preceding paper in this issue.
- (16) Theoretically the χ -parameter of a polymer in a good (athermal) solvent adopts a value of zero. In practice one usually finds for this parameter values of 0.4–0.5. In this work we take the theoretical limiting values of 0 (good solvent) and 0.5 (θ -solvent). See also: Taylor, P. L.; Yu, Y.; Wang, X. Y. *J. Chem. Phys.* **1996**, *105*, 1237.
- (17) Skouri, R.; Schosseler, F.; Munch, J. P.; Candau, S. J. *Macromolecules* **1995**, *28*, 197.
- (18) Rabin, Y.; Panyukov, S. *Macromolecules* **1997**, *30*, 301.
- (19) Weast, R. C.; Astle, M. J., Eds. *CRC Handbook of Chemistry and Physics*, 63rd ed.; CRC Press: Boca Raton, FL, 1982.
- (20) Feynman, R. P.; Leighton, R. B.; Sands, M. *The Feynman Lectures on Physics*, 6th ed.; Addison-Wesley: Reading, MA, 1977; Vol. II, Chapter 38.